

Silanone (Si=O) on Si(100): intermediate for initial silicon oxidationY. J. Chabal,¹ Krishnan Raghavachari,¹ X. Zhang,² and E. Garfunkel²¹*Materials Research, Agere Systems, Murray Hill, New Jersey 07974*²*Department of Chemistry, Rutgers University, Piscataway, New Jersey 08854*

(Received 13 June 2002; published 25 October 2002)

Infrared-absorption measurements and first-principles quantum chemical calculations reveal that the initial oxidation of clean Si(100)-(2×1) by O₂ involves the formation of a metastable silanone intermediate, (O)Si=O, containing two oxygen atoms presumably from the same O₂ molecule. Oxygen insertion into the surface silicon Si-Si backbonds is either thermally activated (~1-eV barrier) or induced by atomic hydrogen exposure with formation of novel dihydride intermediates.

DOI: 10.1103/PhysRevB.66.161315

PACS number(s): 81.65.Mq, 68.43.Fg, 68.43.Pq, 78.55.Ap

To control critical heterointerface properties of future nanoengineered Si-based structures (e.g., high- κ dielectrics and integrated optoelectronics), precise atomic scale knowledge of the growth, structure, and interactions of the Si-O system, including the Si/SiO₂ interface, is necessary. The oxidation mechanism of silicon has been extensively examined for half a century because of its importance in semiconductor device technology.¹⁻⁴ Yet, an atomic level picture of the oxidation mechanism remains elusive. This lack of a thorough mechanistic picture applies to O₂ oxidation of clean Si(100) and (111) surfaces, the H-terminated surfaces, and the SiO₂/Si interface. The initial stages of oxidation of clean Si surfaces by H₂O are somewhat better understood, although an atomic scale model of oxidation beyond the first monolayer remains speculative. Classic O₂ on Si studies that shed some light on the problem have involved vibrational⁵ and electron-loss spectroscopy,⁶ core and valence-band photoemission,⁷⁻⁹ scanning-tunneling microscopy (STM),¹⁰ and theoretical calculations.¹¹⁻¹⁵ What is clear is that there is a strong driving force for O₂ to react and dissociate on Si with an overwhelming propensity to form stable Si-O-Si structures (~9 eV per O₂ molecule downhill), and that these species want to agglomerate to form SiO₂. What remains unresolved is the existence and identity of metastable structures that arise during the reaction of gas phase O₂ with Si to form SiO₂. To date, none of the postulated structures (e.g., physisorbed O₂, peroxide Si-O-O-Si, terminal Si-O, or terminal Si-O-O species) have been definitively observed.

In this paper we present conclusive infrared spectroscopic evidence for the existence of what we argue is a key metastable surface species, silanone (Si=O), observed during O₂ adsorption on Si(100) below room temperature. The assignments of the infrared spectral features are supported by quantum chemical calculations of the vibrational frequencies and total energies of the relevant structures. We demonstrate the conditions under which the silanone species can be created and observed, and present initial results on its thermal and chemical stability.

Samples are cut from double-side polished Si(100) wafers (0.5-mm thick, float zone, 10 Ω cm) that have been thermally oxidized to produce a 3-nm-thick SiO₂ film. Samples are sequentially degreased in trichloroethane, acetone, and isopropanol, then cleaned in 4:1:1 H₂O:H₂O₂:NH₄OH at 80 °C for 10 min, in 4:1:1 H₂O:H₂O₂:HCl at 80 °C for 10 min,

then HF etched (49% HF, 1 min), and finally oxidized with concentrated HNO₃ at 80 °C for 10 min, with profuse rinsing in deionized water between each step. A Si(100) sample is then introduced into an ultrahigh vacuum chamber with two thermocouples attached via tantalum clips to its top and bottom edges. A clean Si(100)-(2×1) surface is obtained by extensive degasing at 600 °C, i.e., below the oxide desorption temperature, followed by a final anneal at 900 °C to remove the thin oxide.¹⁶ Maintaining the base pressure at 9×10^{-11} Torr with liquid N₂-cooled panels ensures that the H₂O residual in the chamber is well below 1×10^{-11} Torr, even during typical O₂ exposures (1–100 L, 1 L $\equiv 10^{-6}$ Torr×sec). Infrared-absorption spectroscopy is performed in transmission with radiation incident at 60° from the surface normal, using Si(100) or O₂ preexposed/annealed surfaces as a reference, as appropriate.¹⁷ Spectra are recorded at low temperatures (153 or 173 K) and annealing sequences consist of 2 min at the annealing temperature, with a 10 K/sec ramp rate.

The surface is modeled by a cluster containing nine silicon atoms to represent the local structure of a single dimer in its immediate environment. The dangling bonds resulting from truncation of Si-Si bonds are terminated by H atoms in order to avoid artifacts due to excess spin or charge. We use a model where the first two layers are allowed to relax fully, while the third and fourth layer atoms in the extended solid are held fixed along ideal bulk crystalline directions (Ref. 4, Chap. 7). The geometry that minimizes the total energy is then obtained for each cluster via gradient corrected density-functional calculations using the B3LYP hybrid functional with a polarized double-zeta basis set. The calculated frequencies are corrected for anharmonicity and other systematic errors by employing simple additive corrections within each mode type.¹⁷⁻¹⁹

Upon O₂ exposure onto a *clean* Si(100)-(2×1) surface at 173 K, an absorption band in the 800–1200-cm⁻¹ range, characteristic of Si-O-Si stretch modes, is observed (Fig. 1) and its intensity increases with exposure. The oxygen coverage of the layer thus formed can be estimated from the integrated area of this band, using data from water oxidation¹⁷ and thin chemical oxide studies.¹⁶ We find $0.07 \pm 0.02\%$ and $0.16 \pm 0.05\%$ ML (1 ML $\equiv 6.8 \times 10^{14}$ cm⁻²) for the 15- and 80-L exposure data shown in Figs. 1(a) and 1(b), respectively (1 L $\equiv 10^{-6}$ Torr×sec). The initial sticking coefficient, as

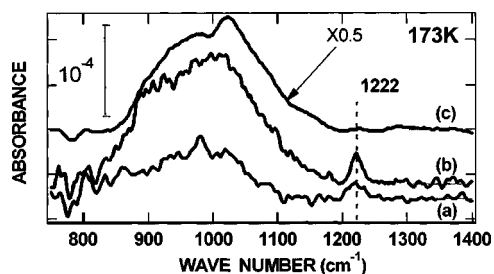


FIG. 1. Infrared-absorption spectra upon O_2 exposure of clean Si(100)-(2 \times 1) at 173 K using the clean surface as reference: (a) 15-L O_2 , (b) 80-L O_2 , and (c) 80-L O_2 with a subsequent anneal to 500 K.

estimated from low exposure data (<15 L), is $s \approx 0.005$. We also note that the oxygen uptake is nonlinear, possibly indicative of Langmuir adsorption behavior. The lack of any observed spectral features in the 600–700-, 2000–2200-, and 3500–3700- cm^{-1} regions, where the Si-H and Si-OH modes of dissociated water occur,¹⁸ confirms that less than 0.01-ML water is adsorbed.

The feature at 1222 cm^{-1} for $^{16}O_2$ [Figs. 1(a) and 1(b)], also observed at 1182.5 cm^{-1} for similar $^{18}O_2$ exposures at 173 K (not shown), is attributed to a silicon-oxygen stretch vibration, but its frequency is unexpectedly high for Si-O-Si modes.²⁰ For all experimentally measured or calculated oxide structures on Si(100), with oxygen either in the dimer bond or the first-to-second layer Si-Si bonds (“backbonds,” for short), the Si-O-Si asymmetric stretch frequencies occur in the 800–1120- cm^{-1} range, including interstitial oxygen atoms in bulk silicon (1105 cm^{-1}). After consideration of several local species such as peroxides, epoxides, and silanones, only silanones, featuring a double bond between Si and O (Si=O), yield vibrational frequencies in this spectral range. Specifically, we calculate the Si=O stretch frequencies at 1164, 1237, and 1295 cm^{-1} for silanone species containing zero, one, and two oxygen atoms in the Si backbonds, respectively. The blueshift induced by backbond oxidation is clearly due to the inductive effect of the electronegative oxygen atoms and has been seen previously in other situations also.^{17,18} Thus the only structure that is consistent with the experimentally observed frequency is silanone containing one oxygen in the backbond [see Fig. 2(a) denoted (O)Si=O], which is reasonable for reactions involving pairs of oxygen atoms such as for O_2 . We note that Si=O has been observed in silica,²¹ porous silicon,^{22–24} and as a diatomic molecule (Si=O) in inert gas matrices²⁵ or physisorbed on Si(111);²⁶ and the frequency we calculate (1295 cm^{-1}) for silanone bonded to two oxygen atoms, (O)₂Si=O, is in excellent agreement with the observed frequency for silanones on the surface of SiO₂ (1306 cm^{-1}).²¹ The calculated isotopic shift on ^{18}O substitution in (O)Si=O yields a frequency shift of 40 cm^{-1} (from 1237 to 1197 cm^{-1}), in excellent agreement with the measured shift of 39.5 cm^{-1} (from 1222 to 1182.5 cm^{-1}). This isotopic shift is distinctly smaller than the value of ~ 50 cm^{-1} predicted for Si-O-Si species resulting from oxygen insertion into the dimer bond or backbonds.

The temperature dependence of the 1222- cm^{-1} feature is

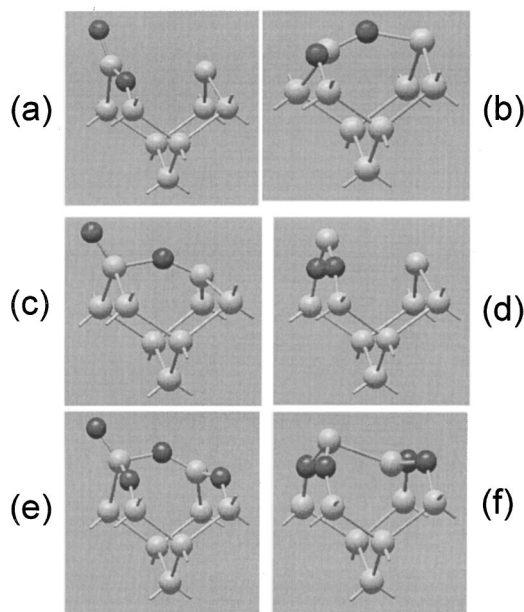


FIG. 2. Schematic diagram of the silanone structures and their corresponding stable oxide structures: (a) “normal” silanone bonding with one oxygen in the backbond, (b) “interacting” silanone bonding with one oxygen in the backbond and dative interaction to the other surface Si atom, (c) two silanone species (one free and the other with a dative interaction) on one dimer unit with no oxygen atoms in the backbonds, (d) oxygen insertion on the same side, (e) two silanone species (one free and the other with dative bonding) on one dimer, each one with an oxygen atom in the backbond, and (f) oxygen insertion on both sides in a four-oxygen dimer unit. Silicon atoms are shown in gray and oxygen atoms in black.

characteristic of a metastable species. Figure 1(c) shows that it disappears upon mild (500-K) annealing, with evidence of oxygen incorporation and rearrangement of the oxide moieties at the surface. While investigating the temperature dependence of the adsorbed oxygen, we noticed that when the surface is preconditioned (partially oxidized) by moderate oxygen exposures at 180 K (20–40 L) followed by 800-K anneals,²⁷ the subsequent adsorption of O_2 and the resulting stabilization of the silanone species are both enhanced (Fig. 3). This is evident in Fig. 3(a) where only 5-L O_2 exposure at 153 K results in three times more oxygen uptake than on a clean surface ($s \approx 0.015$ instead of 0.005) and produces over 10 times more silanone relative to the clean surface at 173 K (based on the 1223- cm^{-1} peak area).

Stability of this silanone intermediate is obtained by looking at its thermal properties summarized in Figs. 3(a)–3(c). The intensity of *three* spectral features at 1001, 1111, and 1223 cm^{-1} have in fact the same temperature dependence and therefore appear to be related to the silanone species formed on oxide-conditioned silicon surfaces. The intensity of all three modes substantially decreases by 350 K, as two new modes appear at 974 and 1018 cm^{-1} [Fig. 3(b)]. The origin of the 1001- and 1111- cm^{-1} modes can be understood by considering a related important structure that also contains the silanone group but involves an additional interaction with the other Si atom of the dimer through a dative bond [Fig. 2(b)]. Though such a structure appears to have an

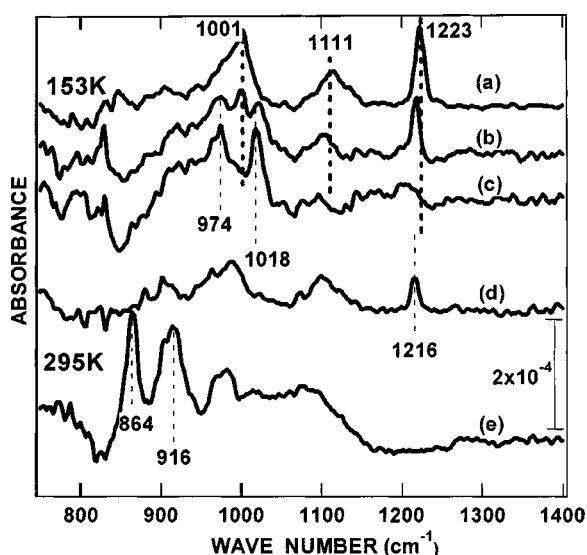


FIG. 3. Infrared-absorption spectra upon O_2 exposure of Si(100)-(2 \times 1) preexposed to oxygen [31 L for series (a)–(c), and 26 L for series (d) and (e)] and preannealed to 915 K. For series (a)–(c), spectra are recorded at 153 K after 2-min anneals at (a) 153, (b) 343, and (d) 523 K. These three spectra are representative of a series of anneals at 50-K intervals between 153 and 523 K. For series (d) and (e), data are recorded and exposures performed at 295 K: (d) initial spectrum, and (e) after 3–4-L atomic H exposure (360-L H_2 with a 2000-K tungsten filament placed 3 cm from the surface). For both series, the reference surface is that of the preexposed/annealed surface, so that the spectra correspond to the absorption associated with 5-L O_2 exposure only.

oxygen inserted into the dimer bond, the two different Si-O bond lengths (~ 1.57 and 1.94 Å) clearly differentiate it from a bridge Si-O-Si by stressing the inequivalence of a strong Si=O bond and a weak, dative Si \leftarrow O bond. The silanone stretching frequency is correspondingly shifted down to ~ 1100 cm^{-1} from this dative interaction while the frequency associated with the oxygen in the backbond position still occurs around 1000 cm^{-1} . We therefore assign the experimentally observed modes at 1111 and 1001 cm^{-1} to such a structure. Another related structure also containing a similar asymmetric interaction (Si-O distances of 1.85 and 1.59 Å) is shown in Fig. 2(c). It is also possible that both species can be present in the same dimer as shown in the structure of Fig. 2(e). Such a species resulting from the interaction of two O_2 molecules in a single dimer is related to a structure considered by Demkov and Sankey,¹³ and reminiscent of the on-top (or “ad-ins”) structures proposed for O_2 adsorption on Si(111)-(7 \times 7).²⁸ Our assignment to two closely related silanone species is consistent with the experimental observation that all three modes disappear together on annealing.

The disappearance of all three modes is not due to desorption, but rather to the insertion of the oxygen atom of the silanone into a surface silicon backbond [Fig. 2(d)]. The transition state for such a process involves an activation barrier of only about 1 eV, in good agreement with what we estimate from the experiment. The resulting structure involves a relatively stable divalent silicon species with two oxygen atoms inserted into the backbonds and has frequen-

cies calculated at 972 and 1035 cm^{-1} , in excellent agreement with the experimentally observed values (974 and 1018 cm^{-1}). In the case of two O_2 molecules in a single dimer unit [Fig. 2(e)], the final structure has a dimer with four oxygen atoms inserted into the backbonds [Fig. 2(f)] and is also characterized by similar frequencies.

Further insight into the reactivity and nature of this metastable silanone species is obtained by examining its interaction with hydrogen. While no spectral change is observed upon 100–500-L *molecular* hydrogen exposure, Figs. 3(d) and 3(e) show that *atomic* hydrogen exposure removes the silanone modes. Note that at room temperature, all three silanone-related modes are relatively weak, due to partial decomposition, and clearly redshifted (now 990, 1100, and 1216 cm^{-1}), due to strong anharmonic coupling to substrate phonons.²⁹ Upon reaction, atomic hydrogen terminates surface dangling bonds, as evidenced by the appearance of vibrational modes at 660, 864, 916 cm^{-1} , 2103, and 2140 cm^{-1} . The modes at 660 and 2103 cm^{-1} (not shown in Fig. 3) along with a weak shoulder at 903 cm^{-1} are well accounted for by dihydride formation on oxygen-free areas of the surface [SiH₂ bend (660), scissor (903), and stretch (2103 cm^{-1})]. In contrast, the modes at 864 and 916 cm^{-1} —linked to the mode at 2140 cm^{-1} —have never been observed previously on clean or oxidized silicon surfaces exposed to atomic hydrogen.

We show that these modes correspond to dihydride species with one and two oxygen atoms in the backbonds, and are a direct consequence of atomic hydrogen interaction with the double-bonded oxygen (Si=O). In a manner similar to H-induced OH decomposition on Si(100),¹⁸ atomic hydrogen interacts with the double-bonded oxygen, to yield radical species that drive the insertion of oxygen into the backbond. The net result is the formation of dihydride structures with oxygen atoms in the backbonds instead of monohydride, as is usually the case, because *two* dangling bonds are liberated as oxygen is inserted into the silicon. Calculations reveal that SiH₂ structures are characterized by wagging modes that are strongly dependent on the number of oxygen atoms in the surface silicon backbonds. For a bare dihydride (without any oxygen), the mode is calculated at 680 and observed at 656 cm^{-1} .¹⁸ In the presence of one and two oxygen atoms in the backbonds of SiH₂, these modes are calculated to shift up to 831 for (O)SiH₂ and 909 cm^{-1} for (O)₂SiH₂, in fairly good agreement with the experimentally observed modes at 864 and 916 cm^{-1} . The corresponding scissor modes of the dihydrides are much weaker (at 931 and 954 cm^{-1}) and cannot be experimentally resolved. The observation of (O)₂SiH₂ results directly from hydrogen-induced migration of the structures of Figs. 2(a) or 2(e), while the (O)SiH₂ species is likely produced from hydrogenation-induced oxygen migration of structures such as those of Figs. 2(b) or 2(c) with each oxygen atom moving to the backbond of the two distinct Si atoms of the dimer. In all cases, dihydrides are formed solely due to the liberation of a double bond upon interaction with Si=O.

The identification and quantification of a silanone intermediate makes it possible to observe that the details of oxygen insertion differ greatly depending on the exact oxidation

conditions. This, in turn, may help explain some apparent discrepancies in the literature. For instance, O₂ exposure of a clean Si(100) initially results in predominantly Si-O-Si formation, with relatively little silanone. In contrast, preoxidation to monolayer levels leads to stabilization of the silanone at similar temperatures, indicating that surface condition, and possibly defects, influence oxidation rates. Furthermore, the large width of the absorption band points to formation of several species in what has become an inhomogeneous surface. These observations confirm the theoretical finding that many “oxide” configurations are energetically equivalent, explain the wide distribution of oxidation states observed in photoemission, are consistent with the lack of ordered structures observed in low-energy electron diffraction and STM, and give us an important new handle on oxidation mechanisms.

The preponderance of the silanone species on preoxidized surfaces indicates that silanone may constitute the main metastable intermediate for oxygen insertion into silicon at low temperatures and gives a clue as to the dominant pathway for an initial oxygen insertion pathway at all temperatures. This information is particularly important because past experimental studies have failed to provide conclusive evi-

dence for any specific proposed intermediate. Previous first-principles calculations have shown that a variety of intermediates with similar total energies can be formed. Many possibilities exist, therefore, possibly involving many different pathways, but the energy barriers between such intermediates that determine the accessibility of the competing reaction pathways are not available in most cases. Under such conditions, we show that it is the combination of experimental *spectroscopic data* recorded over a wide range of temperatures and extensive *calculations* of possible structures with their associated vibrational response and possible reaction pathways that make it possible to unravel the key reactive intermediates. This knowledge has implications well beyond the long-unresolved surface oxidation problem;³⁰ such information must be incorporated, for example, into our developing models of atomic layer deposition of ultrathin gate dielectrics in which the initial oxygen incorporation and subsequently formed interfaces must be controlled at the atomic level.

The authors are grateful to M.K. Weldon and K.T. Queeney for stimulating discussions. X.Z. and E.G. are supported by the Semiconductor Research Corporation.

¹J. T. Law, *J. Phys. Chem. Solids* **4**, 92 (1958).

²E. Irene, *Crit. Rev. Solid State Mater. Sci.* **14**, 175 (1988).

³T. Engel, *Surf. Sci. Rep.* **18**, 91 (1993).

⁴Y. J. Chabal, *Fundamental Aspects of Silicon Oxidation*, edited by A. Zunger, J. R. M. Osgood, R. Hull, and H. Sakati, Springer Series in Materials Science, Vol. 46 (Springer-Verlag, Berlin, 2001).

⁵H. Ibach, H. D. Bruchmann, and H. Wagner, *Appl. Phys. A: Solids Surf.* **29**, 113 (1982).

⁶R. Ludeke and A. Koma, *Phys. Rev. Lett.* **34**, 1170 (1975).

⁷H. Ibach and J. E. Rowe, *Phys. Rev. B* **10**, 710 (1974).

⁸P. Morgen *et al.*, *Phys. Rev. B* **39**, 3720 (1989).

⁹U. Höfer *et al.*, *Phys. Rev. B* **40**, 1130 (1989).

¹⁰I. W. Lyo *et al.*, *J. Phys. Chem.* **94**, 4400 (1990).

¹¹G. F. Cerofolini, G. L. Bruna, and L. Meda, *Appl. Surf. Sci.* **93**, 255 (1996).

¹²K. Kato, T. Uda, and K. Terakura, *Phys. Rev. Lett.* **80**, 2000 (1998).

¹³A. A. Demkov and O. F. Sankey, *Phys. Rev. Lett.* **83**, 2038 (1999).

¹⁴Y. Widjaja and C. B. Musgrave, *J. Chem. Phys.* **116**, 5774 (2002).

¹⁵T. Hoshino *et al.*, *Phys. Rev. B* **50**, 14 999 (1994).

¹⁶Y. J. Chabal *et al.*, *Solid State Phenom.* **65-6**, 253 (1999).

¹⁷B. B. Stefanov *et al.*, *Phys. Rev. Lett.* **81**, 3908 (1998).

¹⁸M. K. Weldon *et al.*, *J. Chem. Phys.* **113**, 2440 (2000).

¹⁹The correction for the Si-O region for the species considered in this paper is -17 cm^{-1} .

²⁰A broad peak centered at $\sim 1220\text{ cm}^{-1}$ was observed almost two decades ago by Ibach, Bruchmann, and Wagner (Ref. 5 above) and assigned to the Si-O-O species. This is ruled out here since our calculations of this species yield a position (1130 cm^{-1}) and an ¹⁸O isotopic shift (65 cm^{-1}), both very different from the experimental observations. For Si-O-Si bonding, LO modes in the $1150\text{--}1250\text{ cm}^{-1}$ range are observed but require much thicker oxides, which is not the case here because the coverage (20% monolayer) is too low for the development of LO modes. Any agglomeration is short range at these temperatures, so that no extended patches can be formed. Furthermore, LO modes would strengthen instead of disappear upon a 200 °C anneal because there is no physical way to quench the LO mode absorption.

²¹V. A. Radsig, V. A. Berestetskaya, and S. N. Kostritsa, *Kinet. Katal.* **39**, 940 (1998).

²²J. L. Gole and D. A. Dixon, *J. Phys. Chem. B* **101**, 8090 (1997).

²³M. V. Wolkin *et al.*, *Phys. Rev. Lett.* **82**, 197 (1999).

²⁴F. Zhou and J. D. Head, *J. Phys. Chem. B* **104**, 9981 (2000).

²⁵R. Withnall and L. Andrews, *J. Phys. Chem.* **89**, 3261 (1985).

²⁶A. J. Schell-Sorokin and J. E. Demuth, *Surf. Sci.* **157**, 273 (1985).

²⁷Such preconditioning results in $>80\%$ clean Si(100)-(2×1), since oxygen atoms are agglomerated into small structures involving two Si-O-Si layers (see Ref. 17).

²⁸S.-H. Lee and M.-H. Kang, *Phys. Rev. Lett.* **82**, 968 (1999).

²⁹R. Honke *et al.*, *Phys. Rev. B* **59**, 10 996 (1999).

³⁰H. Kageshima and K. Shiraiishi, *Surf. Sci.* **380**, 61 (1997).